Receptor-mediated regulation of the TRPM7 channel through its endogenous protein kinase domain

Ryuichi Takezawa*, Carsten Schmitz†‡, Philippe Demeuse*, Andrew M. Scharenberg†, Reinhold Penner*, and Andrea Fleig*§

*Laboratory of Cell and Molecular Signaling, Center for Biomedical Research, The Queen's Medical Center and John A. Burns School of Medicine, University of Hawaii, Honolulu, HI 96813; and †Department of Pediatrics, University of Washington and Children's Hospital and Regional Medical Center, Seattle, WA 98195

TRPM7 is a ubiquitously expressed and constitutively active divalent cation-selective ion channel, whose basal activity is regulated by intracellular levels of Mg^{2+} and Mg·ATP. We have investigated receptor-mediated mechanisms that may actively regulate TRPM7 activity. We here report that TRPM7 currents are suppressed by intracellular GTPγS, suggesting the involvement of heterotrimeric G proteins. TRPM7 currents are also inhibited by stimulating endogenous muscarinic receptors, which is mediated by G_i because the inhibitory effect is blunted by pertussis toxin. Conversely, stimulation of endogenous G_s-coupled β-adrenergic receptors potentiates TRPM7 currents, whereas G_q-coupled thrombin receptors have little effect. Consistent with the involvement of G_s/G_i in controlling adenylyl cyclase activity, elevations of intracellular cAMP levels enhance TRPM7 activity and prevent receptor-mediated modulation of TRPM7 activity by muscarinic and adrenergic agonists. This cAMP-dependent effect requires the functional integrity of both protein kinase A (PKA) and the endogenous kinase domain of TRPM7 because cAMP-mediated effects are abolished when treating cells with the PKA inhibitors H89 or KT5720 as well as in cells expressing phosphotransferase-deficient TRPM7 constructs. These mutant channels are also much less susceptible to GTPγS-mediated inhibition, suggesting that the main regulatory effect occurs through G_i- and G_s-mediated changes in cAMP. Taken together, our results demonstrate that TRPM7 activity is up- and down-regulated through its endogenous kinase in a cAMP- and PKA-dependent manner.

Based on sequence similarities, the mammalian transient receptor potential (TRP) channel family is divided into three subfamilies [TRP classical (formerly short TRP channel)], TRP vanilloid [(formerly osm TRP channel), and TRP melastatin (formerly long TRP channel)] (1–4). TRPM7 (long TRP channel 7, TRP-phospholipase C interacting kinase and channel kinase 1), a Ca^{2+}- and Mg^{2+}-permeable divalent cation channel of the TRP melastatin ion channel subfamily, is required for cellular viability and noted for its ubiquitous distribution profile (5, 6). We have previously demonstrated that TRPM7 is regulated by millimolar levels of intracellular Mg^{2+} and Mg·ATP and its activity appears to be linked to cellular energy metabolism (5, 7). In resting cells, physiological levels of these molecules strongly suppress the activity of TRPM7 channels and only a small constitutive activity remains, sufficient to maintain basal divalent cation fluxes. In whole-cell patch-clamp experiments, intracellular solutions that lack added Mg·ATP lead to activation of TRPM7-mediated currents (Fig. 1*A*) that exhibit a characteristic highly nonlinear current-voltage (I/V) relationship with pronounced outward rectification (Fig. 1*B*). The large outward currents at positive potentials are carried by monovalent ions (e.g., Cs^+ or K^+), whereas the small inward currents at negative potentials are carried by divalent ions such as Ca^{2+} and Mg^{2+}. Although variations in cellular Mg·ATP levels may provide an important "passive" regulatory mechanism of TRPM7, there could be additional "active" mechanisms that control the activity of these channels. One such mechanism has been proposed by

Clapham and coworkers (8), who suggested that phosphatidylinositol bisphosphate may be essential for the function of TRPM7 channels because its depletion after stimulation of G_q-coupled receptors leads to inhibition of TRPM7 currents. The results presented here suggest that TRPM7 activity is primarily modulated by its own kinase domain, responding to changes in intracellular levels of cAMP induced by G_i- and G_s-coupled receptors, respectively.

Methods

Cells. HEK-293 cells transfected with the FLAG-murine TRPM7/pCDNA4/TO construct were grown on glass coverslips with DMEM supplemented with 10% FBS, blasticidin (5 μg/ml), and zeocin (0.4 mg/ml). TRPM7 expression was induced 1 d before use by adding 1 μg/ml tetracycline to the culture medium. Patch-clamp and fura-2 measurements were performed 16–24 h after induction (5). The phosphotransferase activity-deficient point mutant of TRPM7, K1648R, was based on the human TRPM7 construct (9). Endogenous TRPM7-like magnesium–nucleotide-regulated metal ion (MagNuM) currents were measured in HEK-293 transfected with the murine TRPM7 but were not exposed to tetracycline and therefore did not overexpress TRPM7.

Solutions. Cells grown on glass coverslips were transferred to the recording chamber and kept in a standard modified Ringer's solution of the following composition (in mM): NaCl 140, KCl 2.8, $CaCl_2$ 1, $MgCl_2$ 2, glucose 10, and Hepes·NaOH 10, pH 7.2, with osmolarity typically ranging from 298 to 308 mOsm. Intracellular pipette-filling solutions contained (in mM): Cs-glutamate 140, NaCl 8, $MgCl_2$ 1, 1,2-bis(2-aminophenoxy)ethane-N,N,N'-tetraacetic acid tetracaesium salt 10, and Hepes·CsOH, pH 7.2, adjusted with CsOH. In all patch-clamp experiments, free intracellular $[Mg^{2+}]i$ and free $[Ca^{2+}]i$ were adjusted to 780 μM and 100 nM, respectively, by using appropriate mixtures of the chloride salts of these divalent ions as calculated with WEBMAXC 2.1 (http://www.stanford.edu/~cpatton/webmaxc2.htm). In most experiments, 0.3 mM Na·GTP was added, except in experiments with GTPγS and GDPβS. In some experiments, 3 mM Mg·ATP was added as indicated in the text and/or figure legends. Solution changes were performed by pressure ejection from a wide-tipped pipette. Carbachol (CCh), isoproterenol, and thrombin (NaCl-based buffer) were purchased from Sigma.
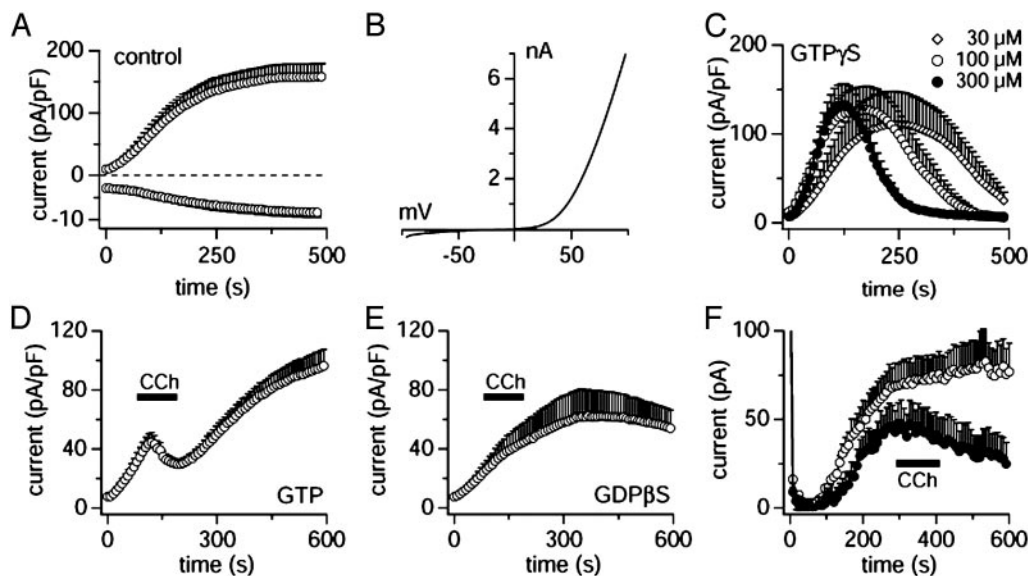
CELL BIOLOGY

Fig. 1. TRPM7 is modulated by G protein-coupled receptors. Whole-cell currents were recorded in HEK-293 cells induced to overexpress murine TRPM7 (*A–E*), except for *F*, which depicts uninduced HEK-293 cells. (*A*) Average inward and outward currents carried by TRPM7 at −80 and +80 mV, respectively (*n* = 5; note the different *y* axis scaling). Cells were perfused with standard internal solution (i.e., with no added Mg·ATP). (*B*) Representative current-voltage (I/V) relationship for fully activated TRPM7, derived from a high-resolution current record in response to a voltage ramp of 50 ms duration that ranged from −100 to +100 mV. (*C*) Cells were perfused with standard internal solution containing various concentrations of GTPγS as indicated in the legend (*n* = 5–11). (*D*) Cells were perfused with standard internal solution containing 0.3 mM GTP (*n* = 6). The bar indicates the time of application of the CCh-containing standard external solution (100 μM). (*E*) Cells were perfused with standard internal solution containing 0.5 mM GDPβS and stimulated by CCh as in *D* (*n* = 5). (*F*) Cells were perfused with standard internal solution as in *D* and stimulated by CCh (●, *n* = 6) or not (○, *n* = 5). MagNuM was inhibited by CCh in 6 of 13 cells (46% of cells).

Calcium Measurements. The cytosolic calcium concentration of individual intact cells was monitored at a rate of 5 Hz with a photomultiplier-based system by using a monochromatic light source tuned to excite fura-2 fluorescence at 360 and 390 nm for 20 ms each (TILL Photonics, Planegg, Germany). Emission was detected at 450–550 nm with a photomultiplier, whose analog signals were sampled and processed by X-CHART software (HEKA Electronics, Lambrecht, Germany). Fluorescence ratios were translated into free intracellular calcium concentration based on calibration parameters derived from patch-clamp experiments with calibrated calcium concentrations. Ester loading of intact cells was performed by incubating cells for 30–45 min in standard solution supplemented with 5 μM fura-2-acetoxymethyl ester.

Patch-Clamp Experiments. Patch-clamp experiments were performed in the tight-seal whole-cell configuration at 21–25°C. High-resolution current recordings were acquired by a computer-based patch-clamp amplifier system (EPC-9, HEKA Electronics). Patch pipettes had resistances between 2 and 4 MΩ after filling with the standard intracellular solution. Immediately after establishment of the whole-cell configuration, voltage ramps of 50 ms duration spanning the voltage range of −100 to +100 mV were delivered from a holding potential of 0 mV at a rate of 0.5 Hz over a period of 300–600 s. All voltages were corrected for a liquid junction potential of 10 mV between external and internal solutions when using glutamate as intracellular anion. Currents were filtered at 2.9 kHz and digitized at 100-μs intervals. Capacitive currents and series resistance were determined and corrected before each voltage ramp by using the automatic capacitance compensation of the EPC-9. The low-resolution temporal development of membrane currents was assessed by extracting the current amplitude at + 80 mV from individual ramp current records. Where applicable, statistical errors of averaged data are given as means ± SEM. with *n*

determinations and statistical significance was assessed by Student's *t* test.

Results and Discussion

TRPM7 Is Inhibited by G Proteins. In an earlier study (5), we have shown that Mg·ATP suppresses heterologously expressed TRPM7 channels as well as MagNuM currents in native systems that exhibit the same current–voltage relationship and regulation by Mg·ATP (5, 7). We also found that MagNuM in rat basophilic leukemia cells was potently inhibited by the nonhydrolysable analog of GTP, GTPγS, indicating that G proteins might be involved in the regulation of TRPM7 (7). To substantiate the role of GTP-binding proteins in TRPM7 activity, we performed experiments with GTPγS in HEK-293 cells overexpressing murine TRPM7. In control experiments with solutions that lack added Mg·ATP (Fig. 1*A*), TRPM7 currents activate quickly and reach a plateau after 200–300 s, whereas intracellular solutions supplemented with various concentrations of GTPγS curtailed the activation and eventually completely inhibited TRPM7 currents (Fig. 1*C*). This effect is dose dependent and TRPM7 currents are progressively inhibited by GTPγS concentrations of 30 μM or higher (10 μM GTPγS was indistinguishable from controls; data not shown). These data suggest that a G protein might be involved in the suppression of TRPM7 activity. Interestingly, however, before this inhibition, GTPγS initially potentiated the activation of TRPM7, hinting at the possibility that there might be a more complex G protein-mediated regulation of TRPM7 that also involves a facilitatory component.

TRPM7 Is Inhibited by Muscarinic Receptor Stimulation. We next wanted to identify the G protein that mediates the inhibitory effect on TRPM7. Our approach was to use G protein-coupled receptors endogenously expressed in HEK-293 cells rather than attempting to overexpress receptors because this can lead to promiscuous G protein coupling (10, 11). We first evaluated the effect of carbachol because HEK-293 cells do express various

muscarinic receptors. As demonstrated in Fig. 1D, the TRPM7 current was significantly inhibited by 100 μM CCh applied extracellularly. After stopping the CCh stimulation, TRPM7 currents increased again, but did not approach the same levels as control currents (compare Fig. 1A; also see Fig. 2B), suggesting that the inhibitory effect on the current was long-lasting. Consistent with the data presented in Fig. 1C, this effect was likely mediated by means of a G protein because no such inhibition was observed in cells perfused with 0.5 mM GDPβS (Fig. 1E). We next wanted to confirm that the receptor-mediated inhibition of TRPM7 was also a feature of native MagNuM currents in uninduced HEK-293 cells. Fig. 1F demonstrates that this is in fact the case in that the native MagNuM current in uninduced HEK-293 cells, except for its smaller magnitude, is very similar to the overexpressed channel (compare Fig. 1A) and is similarly inhibited by ≈50% in cells stimulated with CCh and the inhibition persisted for the duration of the experiment. The somewhat slower kinetics of inhibition may be related to the rather low abundance of TRPM7 channels.

TRPM7 Is Not Inhibited by Phospholipase C (PLC)-Coupled Receptors.
At first sight, these results are compatible with a previous report by Clapham and coworkers (8), who described the inhibition of TRPM7 current by CCh in cells that overexpressed muscarinic M1 receptors. This receptor normally couples to G_q (12) with subsequent PLC activation, and one might therefore conclude that the inhibitory effect of CCh is mediated by means of a G_q-coupled muscarinic receptor (8). We verified that CCh can activate PLC through endogenous receptors in experiments where we monitored $[Ca^{2+}]i$ in uninduced HEK-293 cells. As can be seen in Fig. 2A, CCh is indeed able to produce a Ca^{2+} signal and this result is likely mediated by PLCβ-mediated production of inositol trisphosphate (InsP_3) because the PLC inibitor U73122 completely suppressed the CCh response. However, not all cells responded to CCh (7 of 13 cells tested did not exhibit a visible change in $[Ca^{2+}]i$), and the Ca^{2+} signals of those that did respond (plotted in Fig. 2A) were not very impressive when compared with those generated by, e.g., thrombin (20 units/ml), which produced rapid and large $[Ca^{2+}]i$ signals in 10 of 10 cells tested and therefore appears to be a much stronger agonist for PLC activation in our HEK-293 cells (see Fig. 2A). This prompted us to assess the effect of thrombin on TRPM7 currents, with the expectation to see a strong inhibition of TRPM7. To our surprise, however, thrombin was in fact much less effective than CCh in suppressing TRPM7 currents (Fig. 2B).

We wondered whether the lack of effect of thrombin might be due to some deleterious effect originating from the overexpression of TRPM7. However, thrombin did not affect endogenous MagNuM currents of uninduced HEK-293 cells (Fig. 2C). We next measured the $[Ca^{2+}]i$ responses of cells overexpressing TRPM7. As can be seen in Fig. 2E, in terms of Ca^{2+} signaling, these cells are completely unresponsive to thrombin stimulation and they are also completely unresponsive to CCh. This lack of response must be occurring at some point in the signal transduction pathway between receptor and PLCβ-mediated InsP_3 production because control experiments with pipette-perfused InsP_3 at 20 μM produced normal Ca^{2+} release in TRPM7 overexpressing cells (see Fig. 2F). Because in these cells both CCh and, to a lesser extent, thrombin are still able to inhibit TRPM7 in a G protein-dependent manner, the lack of an InsP_3-mediated Ca^{2+} signal is likely to reside at the level of PLC and we propose that TRPM7 overexpression leads to an inhibition of PLCβ. This proposition is particularly appealing in consideration of the documented ability of TRPM7 to bind to PLC (8).

To further probe the involvement of PLCβ in the regulation of TRPM7, we incubated cells with 10 μM U73122, a potent
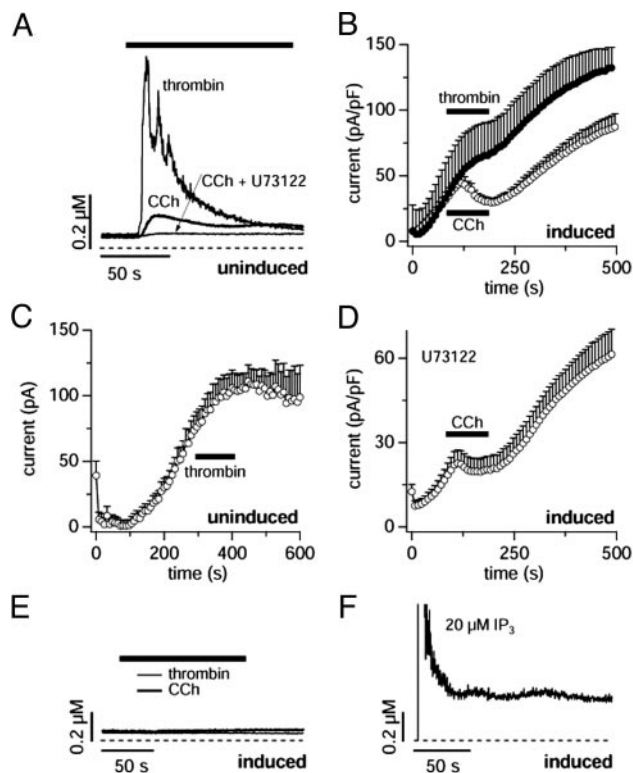

Fig. 2. Receptor-mediated calcium signals do not correlate with TRPM7 regulation. (A) Average calcium signals evoked by CCh (100 μM, $n = 10$) and thrombin (20 units/ml, $n = 10$) in intact, uninduced HEK-293 cells. Cells that did not respond with a change in $[Ca^{2+}]i$ were omitted. Preincubation of cells with the PLC inhibitor U73122 (10 μM, $n = 10$) abolished CCh responses. (B) Current amplitudes evoked by the standard ramp protocol recorded at +80 mV in HEK-293 cells overexpressing TRPM7. The bar indicates the time of application of either thrombin (20 units/ml) or CCh (100 μM). Thrombin has only mild inhibitory effects on TRPM7 currents (●, $n = 9$) as compared with CCh (○, same data as in Fig. 1C). (C) Current amplitudes evoked by the standard ramp protocol recorded at +80 mV in uninduced HEK-293 cells as in Fig. 1F. The bar indicates the time of application of thrombin (20 units/ml), with no significant effect on MagNuM ($n = 10$). (D) Current amplitudes evoked by the standard ramp protocol recorded at +80 mV in HEK-293 cells overexpressing TRPM7 and preincubated with U73122 (10 μM, $n = 11$). The bar indicates the time of application of CCh (100 μM). Note that the PLC inhibitor did not suppress the CCh-mediated inhibition of TRPM7. (E) Average calcium signals evoked by CCh (100 μM, $n = 10$) and thrombin (20 units/ml, $n = 10$) in intact, tetracycline-induced HEK-293 cells overexpressing TRPM7. Note the complete absence of calcium release with either agonist. (F) Average calcium signals evoked by intracellular InsP_3 (20 μM, $n = 3$) in intact, tetracycline-induced HEK-293 cells overexpressing TRPM7. Note that InsP_3-induced calcium release and subsequent store-operated Ca^{2+} influx is not compromised.

inhibitor of this enzyme. As expected, this completely abolished the CCh-induced Ca^{2+} signal (Fig. 2A). U73122 has been reported to have a direct pharmacological effect on TRPM7 currents (8), and we also observed this direct effect of U73122. However, the inhibition of TRPM7 current by 10 μM U73122 was only ≈50% and therefore still allows one to assess the efficacy of CCh in modulating TRPM7. As can be seen in Fig. 2D, the inhibitory effect of CCh on TRPM7 in the presence of U73122 remains largely unaffected. From these results it appears that PLC stimulation and phosphatidylinositol bisphosphate depletion may not be the mechanism that accounts for the TRPM7 inhibition by means of endogenous muscarinic receptors we observe.

TRPM7 Is Inhibited by Pertussis Toxin (PTX)-Sensitive G Proteins.
Based on the above results, we reasoned that the CCh-mediated inhibition of TRPM7 was likely mediated by either of two G

CELL BIOLOGY
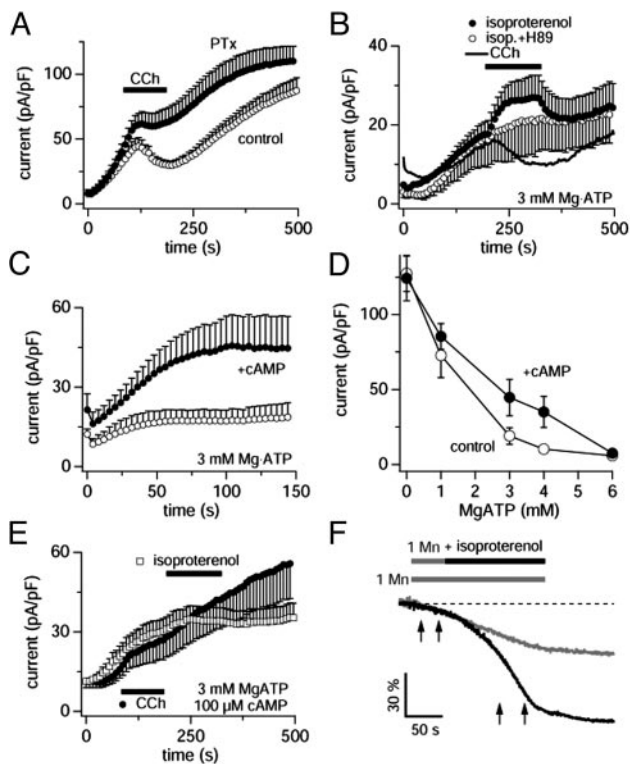
Fig. 3. TRPM7 is inhibited by G_i and facilitated by cAMP. Data are derived from whole-cell outward currents recorded at +80 mV in HEK-293 cells overexpressing TRPM7. (*A*) Cells were pretreated with 1 μg/ml PTX for 4–7 h, perfused with standard internal solution containing 0.3 mM GTP, and stimulated by 100 μM CCh (●, $n = 7$). The currents measured in PTX-untreated cells are shown as control (○, same data as in Fig. 1*D*). (*B*) Average whole-cell currents in cells perfused with 3 mM Mg·ATP and stimulated with 100 μM CCh (line plot, $n = 5$) as well as 300 μM isoproterenol in the presence (○, $n = 5$) or absence (●, $n = 5$) of 10 μM H89 in the internal solution. Note that H89 completely abolishes isoproterenol-mediated facilitation of TRPM7. The H89 data have been shifted by -8 pA/pF for display purposes. (*C*) Average whole-cell currents in cells perfused with intracellular solutions containing 3 mM Mg·ATP alone (○, $n = 8$) or additionally 100 μM cAMP (●, $n = 8$). Note the strong facilitation of TRPM7 currents by cAMP. (*D*) Data points correspond to averaged and normalized current amplitudes measured at +80 mV after 300 s of whole-cell recording, plotted as a function of intracellular Mg·ATP concentrations ($n = 7$–15). Current amplitudes evoked in the absence (○) and presence (●) of 100 μM intra-pipette cAMP. The data points at 3 and 4 mM Mg·ATP are statistically significant with $P < 0.03$ as determined by Student's paired t test. (*E*) Average whole-cell currents in cells perfused with intracellular solutions containing 3 mM Mg·ATP and 100 μM cAMP. Extracellular application of either 100 μM CCh (●, $n = 11$) or 300 μM isoproterenol (□, $n = 8$) now fail to modulate TRPM7 currents. (*F*) Typical examples of fluorescence quench of fura-2 fluorescence induced by Mn^{2+} in HEK-293 cells overexpressing TRPM7 in the absence (gray trace) or additional presence of 300 μM isoproterenol. The rate of Mn^{2+}-induced quench of fura-2 during the time indicated by the first pair of arrows was $32 \pm 8\%$/min ($n = 5$), and cells that were exposed to isoproterenol had average rates of $76 \pm 6\%$/min ($n = 5$) during the time indicated by the second set of arrows.

proteins that muscarinic receptors preferentially engage (12), namely G_q (muscarinic receptor types 1, 3, and 5) and G_i/G_o (muscarinic receptor types 2 and 4). To determine whether G_i was responsible for the modulation of TRPM7 activity, we pretreated HEK-293 cells overexpressing TRPM7 for 4–7 h with PTX (1 μg/ml), a toxin inhibitor of G_i. In PTX-treated cells, application of CCh was significantly less effective in suppressing TRPM7 currents (Fig. 3*A*), although some mild inhibition remained. Thus, assuming that muscarinic receptors signal exclusively through G_q and G_i/G_o, a large part of the CCh effect

appears to be mediated through G_i and the remaining suppression could either be due to residual G_i activity as a result of incomplete PTX block and/or additional direct suppression of TRPM7 by G_q. The latter possibility of a residual G_q-mediated effect appears quite attractive because it would be compatible with the small inhibitory effects we observed with thrombin (see Fig. 2*B*). Although thrombin is known to couple to a range of other heterotrimeric G proteins (13, 14) (including G_i, $G_{12/13}$, and G_o), judging from the very strong Ca^{2+} signal induced by this agonist (see Fig. 2*A*), G_q may well represent the predominant effector G protein of thrombin in our HEK-293 cells.

TRPM7 Is Modulated by cAMP and PKA. We next asked whether the G_i-mediated inhibition was a direct G protein effect or secondary to the downstream effectors of G_i. Because engagement of G_i reduces intracellular levels of cAMP by inhibiting adenylyl cyclase, the G_i-mediated suppression of TRPM7 could be an indirect action through a reduction in cAMP and a concomitant decrease in PKA activity, which when paired with constitutive phosphatase activity, would result in decreased phosphorylation levels and decreased TRPM7 activity. The opposite would be expected for stimuli that increase cAMP levels. To address this issue, we tested for possible modulatory effects of β-adrenergic receptors, which normally couple to G_s and elevate cellular cAMP. To this end, we perfused HEK-293 cells overexpressing TRPM7 with solutions that contained physiological levels of Mg·ATP (3 mM) and stimulated them by isoproterenol (300 μM), a specific agonist of β-adrenergic receptors (Fig. 3*B*). As can be seen, this resulted in a significant potentiation of TRPM7 currents, suggesting that receptor-mediated changes in TRPM7 activity might indeed be determined by cAMP, which is produced by adenylyl cyclase, an enzyme that is activated by G_s and inhibited by G_i. Conversely, CCh produced a significant inhibition of TRPM7 under these conditions, again compatible with a G_i-mediated inhibition of adenylyl cyclase. Because the immediate downstream effector system of adenylyl cyclase-induced increases in cAMP is PKA, we performed experiments where PKA activity was suppressed by two of its inhibitors, H-89 (15) and KT5720 (16), which we perfused into cells at 10 and 1 μM concentration, respectively. When exposed to either of these inhibitors, TRPM7 developed normally, but isoproterenol was no longer able to increase its activity (H89 effects are illustrated in Fig. 3*B*; KT5720 effects were identical, data not shown), suggesting that TRPM7 activity is indeed up-regulated secondary to PKA stimulation.

To confirm and further evaluate the effect of cAMP in the regulation of TRPM7, we performed experiments with cAMP and its membrane-permeable analog dibutyryl-cAMP to directly increase cAMP levels in the absence of receptor stimulation. As can be seen in Fig. 3*C*, pipette-perfused cAMP (100 μM) significantly enhanced TRPM7 activity compared with controls. Likewise, extracellular application of the membrane-permeable dibutyryl-cAMP (5 mM) reversibly enhanced TRPM7 currents (data not shown, but see Fig. 4*A*), and this facilitatory effect was again completely suppressed by H-89 (data not shown). As TRPM7 itself contains a kinase domain (5, 6, 17), we evaluated the effects of cAMP and H89 on TRPM7 kinase activity *in vitro* and observed neither enhancement nor diminution of kinase activity by either reagent (data not shown). Therefore, the above results are most consistent with cAMP-dependent facilitation of TRPM7 mediated by PKA.

The above experiments probing the TRPM7 facilitation were all performed at near physiological intracellular levels of Mg·ATP (3 mM). We also assessed the Mg·ATP dependence of the cAMP-mediated facilitation of TRPM7 by perfusing cells with intracellular solutions containing 100 μM cAMP and different concentrations of Mg·ATP. Fig. 3*D* illustrates this dependency and demonstrates that the cAMP-mediated facili-
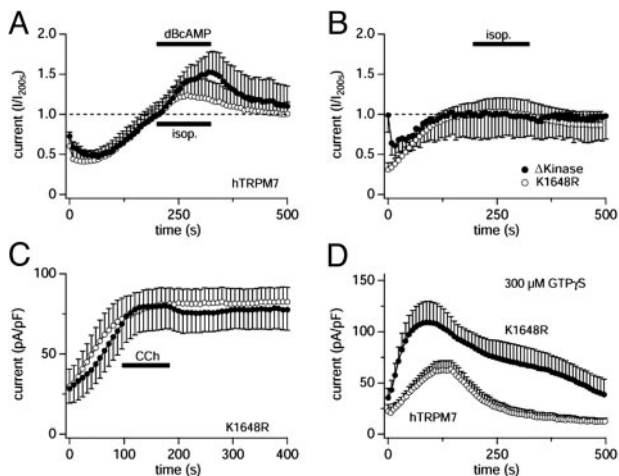
Fig. 4. Receptor-mediated regulation of TRPM7 is mediated by the kinase domain. Data are from HEK-293 cells overexpressing various constructs of human TRPM7. (*A*) Normalized average whole-cell currents at +80 mV (current amplitudes at 200 s were set to 1) in cells overexpressing WT hTRPM7 perfused with intracellular solutions containing 3 mM Mg·ATP (plus 0.3 mM GTP in the case of receptor stimulation) and stimulated by 300 μM isoproterenol ($\bigcirc$, n = 6) or exposed to extracellular solution containing 5 mM dibutyryl-cAMP ($\bullet$, n = 5). Note that both stimuli induce facilitation in hTRPM7. (*B*) Normalized average whole-cell currents at +80 mV (current amplitudes at 200 s were set to 1) in HEK-293 cells overexpressing phosphotransferase-deficient constructs caused by either a single point mutation of hTRPM7 (K1648R) or C-terminal truncation of the kinase domain of hTRPM7 (Δ-kinase) and stimulated by 300 μM isoproterenol. K1648 cells were perfused with intracellular solutions containing 3 mM Mg·ATP and 0.3 mM GTP ($\bigcirc$, n = 5). Δ-Kinase cells were perfused with intracellular solutions with reduced free MgCl₂ (calculated free Mg^{2+} of 216 μM) containing 3 mM Na·ATP, 0.3 mM GTP, and free [Ca^{2+}]i buffered to 100 nM ($\bullet$, n = 5). Note that isoproterenol-induced facilitation is abolished in both phosphotransferase-deficient constructs. (*C*) Currents recorded from K1648R cells with the same experimental protocol as in *A* and stimulated with 100 μM CCh ($\bullet$; n = 7) or not ($\bigcirc$; n = 4). Note that CCh-induced inhibition normally observed in TRPM7 WT (see Fig. 1*D*) is almost completely abolished in the K1648R mutant. (*D*) Same experimental protocol as in Fig. 1*A*. K1648R-overexpressing HEK-293 cells were perfused with the standard internal solution containing 300 μM GTPγS ($\bullet$, n = 5). For comparison, the graph also plots WT human TRPM7 perfused with the same solution ($\bigcirc$, n = 6). Note that inhibitory effects of GTPγS are greatly reduced in the K1648R mutant.

tation is gradually reduced when lowering Mg·ATP levels and completely lost when Mg·ATP is close to zero. At higher levels of Mg·ATP (6 mM), there is no obvious facilitation, because Mg·ATP itself acts as an inhibitor of TRPM7 (5). Thus, the main facilitatory of cAMP is observed at physiological levels of Mg·ATP of 3–4 mM, where it amounts to as much as 100% increase in current amplitude. To further demonstrate the specificity of the cAMP-mediated effect, we performed experiments in which we perfused cells with 100 μM cAMP and 3 mM Mg·ATP, where we expect maximal stimulation of PKA, and then challenged these cells by both isoproterenol and CCh. Under these conditions, the agonists would be expected to be ineffective because a supramaximal concentration of cAMP is already supplied by means of the patch pipette. Indeed, Fig. 3*E* illustrates that under these conditions, both agonists fail to induce additional modulatory effects on TRPM7.

Finally, we reasoned that this modulatory effect of receptor-mediated enhancement of TRPM7 activity should also be manifest in intact cells. We took advantage of the fact that TRPM7 is able to transport virtually all divalent metal ions (18), including Mn^{2+}, and measured Mn^{2+} entry in HEK-293 through Mn^{2+}-mediated quenching of fura-2. Fig. 3*F* illustrates typical changes in fura-2 fluorescence in a cell that was exposed to 1 mM Mn^{2+}

alone (gray trace) as well as an example of a cell that was first exposed to Mn^{2+} alone and then to Mn^{2+} plus isoproterenol (black trace). As can be seen, isoproterereneol induced a strong acceleration in the rate of Mn^{2+} entry compared with control cells exposed to Mn^{2+} alone, indicating that the receptor-mediated modulation of TRPM7 also occurs in intact cells.

TRPM7 Regulation by cAMP/PKA Requires a Functional TRPM7 Kinase Domain. We have recently demonstrated that phosphotransferase activity-deficient mutants of TRPM7 exhibit altered Mg^{2+}- and Mg·ATP-dependent suppression of basal channel activity (9). To determine whether active regulation of TRPM7 is also mediated through the TRPM7 kinase domain, we compared the effects of GPCR activation on whole cell currents produced after expression of human TRPM7 (hTRPM7), a phosphotransferase activity-deficient point mutant (K1648R), and a kinase-domain deletion mutant (Δ-kinase). Fig. 4*A* illustrates that both isoproterenol and dibutyryl-cAMP induce a reversible facilitation of overexpressed WT hTRPM7 currents, which is identical to that observed for murine TRPM7, complementing experiments that demonstrate inhibitory effects of CCh on endogenous MagNuM of human HEK-293 cells (see Fig. 1 *D* and *F*). Both the K1648R and Δ-kinase constructs result in functional hTRPM7 channels that no longer exhibit any significant kinase activity but remain regulated by free [Mg^{2+}]i and Mg·ATP (9); however the basal activity of the Δ-kinase mutant is considerably more sensitive to inhibition by Mg·ATP than the WT channel and the basal activity of the K1648R mutant significantly less so. Although the latter construct could be tested under the same experimental conditions as those used for the murine and human versions of WT TRPM7 (see, e.g., Fig. 3*B*), the Δ-kinase mutant is completely suppressed at 3 mM Mg·ATP (9). We therefore used lower Mg·ATP and Mg^{2+} concentrations (see figure legend for details) to test for isoproterenol-induced facilitation of TRPM7-Δ-kinase activity and verified that such a regulation was present in the WT hTRPM7 under these conditions (data not shown). As illustrated in Fig. 4*B*, both the K1648R and Δ-kinase mutants of hTRPM7 are completely resistant to isoproterenol-mediated facilitation, suggesting that receptor-mediated potentiation of the WT channel is intrinsic to TRPM7 and dependent on the functional kinase domain of the channel. Similarly, CCh, which under similar experimental conditions strongly inhibits TRPM7 (see Fig. 3*B*), no longer showed a significant inhibition in HEK-293 cells expressing the K1648R hTRPM7 construct (Fig. 4*C*), suggesting that the dysfunctional kinase domain can no longer translate cAMP changes into altered channel activity.

In light of the above experiments, we can also conclude that much of the GTPγS-induced inhibition of TRPM7 (see Fig. 1*C*) is mediated predominantly through G$_i$, which apparently overpowers the stimulatory action through G$_s$; although the latter may account for the initial facilitation observed at high GTPγS concentrations. It is possible that the overall inhibition by GTPγS may also be supported by other G proteins including G$_q$ because both CCh and thrombin retained mild inhibitory effects in cells treated with PTX. From this, one would expect the K1648R mutant channels to be less strongly inhibited by GTPγS because the inhibitory action of G$_i$ would be missing and leave only the mild inhibition through other G proteins. The experiments in Fig. 4*D* illustrate that this is indeed what can be observed experimentally when perfusing K1648R expressing cells with a saturating dose of GTPγS (300 μM). When comparing the effects of GTPγS on WT hTRPM7 and K1648R channels, the currents carried by the K1648R mutant clearly are significantly less sensitive to GTPγS. These data are consistent with the interpretation that TRPM7 is primarily regulated by its endogenous kinase domain responding to changes in cAMP levels, brought about by G$_i$ and G$_s$ proteins through regulation of adenylyl cyclase. In addition, a smaller inhibitory signal may

be provided by other G proteins, possibly G_q, which may occur through more direct interaction with the channel.

Conclusion

In summary, the present study provides an unique mechanism for regulation of TRPM7 activity where receptor-mediated changes in cAMP levels, which control the activity of PKA, are translated through the endogenous kinase domain of TRPM7 into altered channel activity. In contrast to previous work by Clapham and coworkers (8), who suggested that phosphatidylinositol bisphosphate depletion is responsible for the receptor-mediated inhibition of TRPM7, our present study finds no evidence for such a mechanism. In fact, overexpression of TRPM7 in our hands leads to a complete suppression of PLC-mediated signaling and likely abolishes any phosphatidylinositol bisphosphate breakdown, without affecting the receptor-mediated regulation of TRPM7. Our previous work has demonstrated that, whereas the endogenous kinase domain of TRPM7 is not essential for the gating of the channel (5, 9), it will

affect the "passive" sensitivity of the channel to both free Mg^{2+} and Mg·ATP (9). The present study now demonstrates an "active" regulatory mechanism that will increase or decrease TRPM7 activity based on receptor-mediated changes in cAMP levels. Although the Mg·ATP-mediated regulation and the cAMP-dependent modulation of TRPM7 may be two separate and unrelated mechanisms, it is also possible that they may be linked. For example, the cAMP-induced activation of PKA could induce a shift in Mg·ATP sensitivity of TRPM7 or conversely, changes in Mg·ATP could determine the activity of PKA and the endogenous kinase activity of TRPM7. Taken together, these results suggest that the role of TRPM7 in cellular ion homeostasis is due to its ability to integrate metabolic and receptor-mediated influences on the transport of divalent metal ions.

1. Clapham, D. E., Runnels, L. W. & Strubing, C. (2001) *Nat. Rev. Neurosci.* **2,** 387–396.
2. Harteneck, C., Plant, T. D. & Schultz, G. (2000) *Trends Neurosci.* **23,** 159–166.
3. Montell, C., Birnbaumer, L., Flockerzi, V., Bindels, R. J., Bruford, E. A., Caterina, M. J., Clapham, D. E., Harteneck, C., Heller, S., Julius, D., *et al.* (2002) *Mol. Cell* **9,** 229–231.
4. Montell, C., Birnbaumer, L. & Flockerzi, V. (2002) *Cell* **108,** 595–598.
5. Nadler, M. J., Hermosura, M. C., Inabe, K., Perraud, A. L., Zhu, Q., Stokes, A. J., Kurosaki, T., Kinet, J. P., Penner, R., Scharenberg, A. M., *et al.* (2001) *Nature* **411,** 590–595.
6. Runnels, L. W., Yue, L. & Clapham, D. E. (2001) *Science* **291,** 1043–1047.
7. Hermosura, M. C., Monteilh-Zoller, M. K., Scharenberg, A. M., Penner, R. & Fleig, A. (2002) *J. Physiol. (London)* **539,** 445–458.
8. Runnels, L. W., Yue, L. & Clapham, D. E. (2002) *Nat. Cell Biol.* **4,** 329–336.
9. Schmitz, C., Perraud, A. L., Johnson, C. O., Inabe, K., Smith, M. K., Penner, R., Kurosaki, T., Fleig, A. & Scharenberg, A. M. (2003) *Cell* **114,** 191–200.
10. Tucek, S., Michal, P. & Vlachova, V. (2002) *Trends Pharmacol. Sci.* **23,** 171–176.
11. Kenakin, T. (1996) *Pharmacol. Rev.* **48,** 413–463.
12. Caulfield, M. P. & Birdsall, N. J. (1998) *Pharmacol. Rev.* **50,** 279–290.
13. Vanhauwe, J. F., Thomas, T. O., Minshall, R. D., Tiruppathi, C., Li, A., Gilchrist, A., Yoon, E. J., Malik, A. B. & Hamm, H. E. (2002) *J. Biol. Chem.* **277,** 34143–34149.
14. Gilchrist, A., Vanhauwe, J. F., Li, A., Thomas, T. O., Voyno-Yasenetskaya, T. & Hamm, H. E. (2001) *J. Biol. Chem.* **276,** 25672–25679.
15. Chijiwa, T., Mishima, A., Hagiwara, M., Sano, M., Hayashi, K., Inoue, T., Naito, K., Toshioka, T. & Hidaka, H. (1990) *J. Biol. Chem.* **265,** 5267–5272.
16. Kase, H., Iwahashi, K., Nakanishi, S., Matsuda, Y., Yamada, K., Takahashi, M., Murakata, C., Sato, A. & Kaneko, M. (1987) *Biochem. Biophys. Res. Commun.* **142,** 436–440.
17. Yamaguchi, H., Matsushita, M., Nairn, A. C. & Kuriyan, J. (2001) *Mol. Cell* **7,** 1047–1057.
18. Monteilh-Zoller, M. K., Hermosura, M. C., Nadler, M. J., Scharenberg, A. M., Penner, R. & Fleig, A. (2003) *J. Gen. Physiol.* **121,** 49–60.

Takezawa *et al.*